


2005

# The Influence of Lipid Composition on the Binding of LDL to Chondroitin 6-Sulphate

Wilma Espiritu

*Virginia Commonwealth University*

Follow this and additional works at: <http://scholarscompass.vcu.edu/etd>

 Part of the [Biochemistry, Biophysics, and Structural Biology Commons](#)

© The Author

---

Downloaded from

<http://scholarscompass.vcu.edu/etd/943>

This Thesis is brought to you for free and open access by the Graduate School at VCU Scholars Compass. It has been accepted for inclusion in Theses and Dissertations by an authorized administrator of VCU Scholars Compass. For more information, please contact [libcompass@vcu.edu](mailto:libcompass@vcu.edu).

© © Wilma O. Espiritu 2005

All Rights Reserved

THE INFLUENCE OF LIPID COMPOSITION ON THE BINDING OF LDL TO  
CHONDROITIN 6-SULPHATE

A Thesis submitted in partial fulfillment of the requirements for the degree of Master of  
Science in Biochemistry at Virginia Commonwealth University.

by

WILMA O. ESPIRITU  
Bachelor of Science in Psychology,  
Virginia Polytechnic Institute and State University, 2000

Director: RIK VAN ANTWERPEN, PH.D.  
ASSISTANT PROFESSOR, DEPARTMENT OF BIOCHEMISTRY

Virginia Commonwealth University  
Richmond, Virginia  
November, 2005

### Acknowledgement

I would like to thank a few people for making this effort possible. First of all, Dr. Rik van Antwerpen for giving a chance in realizing my future endeavors. The faculty and students of the department of Biochemistry in the Medical College of Virginia, VCU, had embraced me into their program. To my lab mates, we never had a dull moment. Christopher Tagliente, who had given me endless moral support and encouragement, because of him I was never alone during the many late nights working in the lab. And finally, to my parents, Wilfredo and Preciosa Espiritu, they have always believed in me and my abilities even when I thought I was falling short. I would not be where I am today without the love and support of my family and friends. Thank you for your undying support.

## Table of Contents

	Page
Acknowledgements .....	ii
List of Figures.....	v
 Chapter	
1 Introduction .....	1
1.1 Response-to-Injury Hypothesis.....	1
1.2 Oxidative Modification Hypothesis .....	2
1.3 Response-to-Retention Hypothesis .....	3
1.4 Proteoglycans and Glycosaminoglycans.....	6
1.5 Lipoprotein Production and Cholesterol Metabolism.....	10
1.6 Low-Density Lipoproteins .....	11
1.7 LDL's Function in the Body .....	14
1.8 Low-Density Lipoprotein – Glycosaminoglycan Interaction .....	14
1.9 Physical State of the LDL Core .....	15
1.10 Hypothesis.....	16
2 Materials and Methods .....	17
2.1 Isolation of Lipoproteins.....	17
2.2 Compositional Analysis .....	19
2.3 Sodium Dodecyl Sulphate Polyacrylamide Gel Electrophoresis (SDS- PAGE).....	19

2.4	Differential Scanning Calorimetry (DSC) .....	20
2.5	Electrophoretic Mobility Shift Gels .....	21
2.6	Spectrophotometric Determination of Conjugated Dienes .....	21
2.7	LDL-C6S Turbidity Binding Assays .....	22
2.8	Statistical Analysis .....	22
2.9	Nuclear Magnetic Resonance Analysis – LipoScience, Inc. ....	23
3	Results .....	26
3.1	Physicochemical Characteristics of LDL .....	26
3.1.1	Lipid Composition .....	26
3.1.2	Level of Oxidation .....	29
3.1.3	Phase Transition Temperature of LDL .....	29
3.2	LDL:C6S Complex Formation.....	31
3.3	Phase Transition Temperature of the LDL Core and C6S Binding .....	36
3.4	LDL Lipid Composition and C6S Binding .....	38
4	Discussion.....	45
4.1	Particle Size: Small versus Large.....	45
4.2	Arterial Proteoglycans versus Purified Glycosaminoglycans .....	47
	References .....	50

## List of Figures

	Page
Figure 1: Early Stages of Atherogenesis .....	5
Figure 2: Proteoglycans and Glycosaminoglycans.....	8
Figure 3: How Glycosaminoglycans are Linked to the Protein Core of Proteoglycans.....	9
Figure 4: Low-density Lipoprotein.....	13
Figure 5: NMR LipoProfile® Report (Page 1).....	24
Figure 6: NMR LipoProfile® Report (Page 2).....	25
Figure 7: Compositional Analysis LDL .....	28
Figure 8: Phase Transition Temperatures.....	30
Figure 9: Chondroitin 6-Sulphate Turbidity Assays.....	33
Figure 10: Particle Number versus Aggregation Size .....	35
Figure 11: Maximal Binding of LDL to C6S .....	37
Figure 12: Maximal Binding of LDL to C6S versus Lipid Composition.....	40
Figure 13: Lipid Composition versus Particle Size .....	42
Figure 14: Maximal C6S Binding, Lipid Content, and LDL Size.....	44

## Abstract

### THE INFLUENCE OF LIPID COMPOSITION ON THE BINDING OF LDL TO CHONDROITIN 6-SULPHATE

By Wilma O. Espiritu, M.S.

Thesis submitted in partial fulfillment of the requirements for the degree of Master of  
Science in Biochemistry at Virginia Commonwealth University.

Virginia Commonwealth University, 2005

Major Director: Rik van Antwerpen, Ph.D.  
Assistant Professor, Department of Biochemistry

The interaction between low-density lipoprotein (LDL) and glycosaminoglycans is a key factor in atherosclerosis. The present study examines the characteristics of LDL and its binding properties with the main glycosaminoglycan of the vascular wall, chondroitin 6-sulphate (C6S). The compositional characteristics that were studied for each LDL sample were phase transition temperature, phospholipid content, free cholesterol content, cholesteryl ester content, triglyceride content, and size. Correlations of these characteristics with LDL-C6S binding were analyzed using a turbidity assay. Our results showed that there is no correlation between LDL-C6S binding and phase transition



temperature, triglyceride content, or size. Strong correlations were present for LDL-C6S binding and phospholipid content ( $P < 0.0001$ ,  $r^2 = 0.4591$ ), free cholesterol content ( $P < 0.01$ ,  $r^2 = 0.2495$ ), and cholesteryl ester content ( $P < 0.005$ ,  $r^2 = 0.2952$ ). When values for surface (phospholipids and free cholesterol) and core (cholesteryl esters and triglycerides) lipids were determined a positive correlation was also present with LDL-C6S binding ( $P < 0.0005$ ,  $r^2 = 0.4172$ ;  $P < 0.0005$ ,  $r^2 = 0.4282$ ; respectively). These results indicate that large, lipid-rich LDL particles have a higher capacity to bind C6S than smaller, lipid poor LDL. Possible implications for the atherogenicity of LDL are discussed.

## **CHAPTER 1 INTRODUCTION**

Atherosclerosis is a systemic disease that is characterized by the accumulation of lipid-rich plaques within the walls of large arteries. The major clinical outcomes of atherosclerosis are well known and include coronary heart disease, stroke, and peripheral vascular disease. It is the leading cause of mortality in men and women in modern nations.<sup>1</sup> Because of this fact, it is important to examine what the key factors are, how they become malicious, and what can be done to prevent or even eliminate the known outcomes.

Starting from as early as the fetus,<sup>2</sup> atherosclerotic lesions are formed and develop basically in three stages: endothelial dysfunction, fatty streak formation, and fibrous cap formation. Through the years three major atherosclerosis hypotheses have emerged to provide a starting point. They are the response-to-injury hypothesis, the oxidative modification hypothesis, and the response-to-retention hypothesis.

### **1.1 Response-to-Injury Hypothesis**

Ross and Glomset proposed the response-to-injury hypothesis in the 1990s and pointed to endothelial dysfunction as a critical factor.<sup>3</sup> Endothelial injury can be caused by key risk factors which can be genetic and/or environmental, for example, elevated levels of cholesterol and triglyceride in the blood, high blood pressure, cigarette smoke, and

viruses.<sup>4</sup> The hypothesis suggests that an endothelial injury initiates a cascade of responses that alter normal vascular homeostasis. Because of this endothelial dysfunction there is enhanced endothelial permeability and deposition of LDL particles in the intima. This also triggers leukocyte adhesion and transmigration across the endothelium. Soon after, inflammatory responses such as T-cell activation, platelet adherence and aggregation, and additional entry of leukocytes, smooth muscle cell migration and proliferation occur. After monocytes differentiate into macrophages they are able to take in LDL and form “foam cells”. The final steps in this hypothesis involve continued foam cell formation, fibrous cap formation, and necrosis in the core of the lesion.<sup>5</sup>

## **1.2 Oxidative Modification Hypothesis**

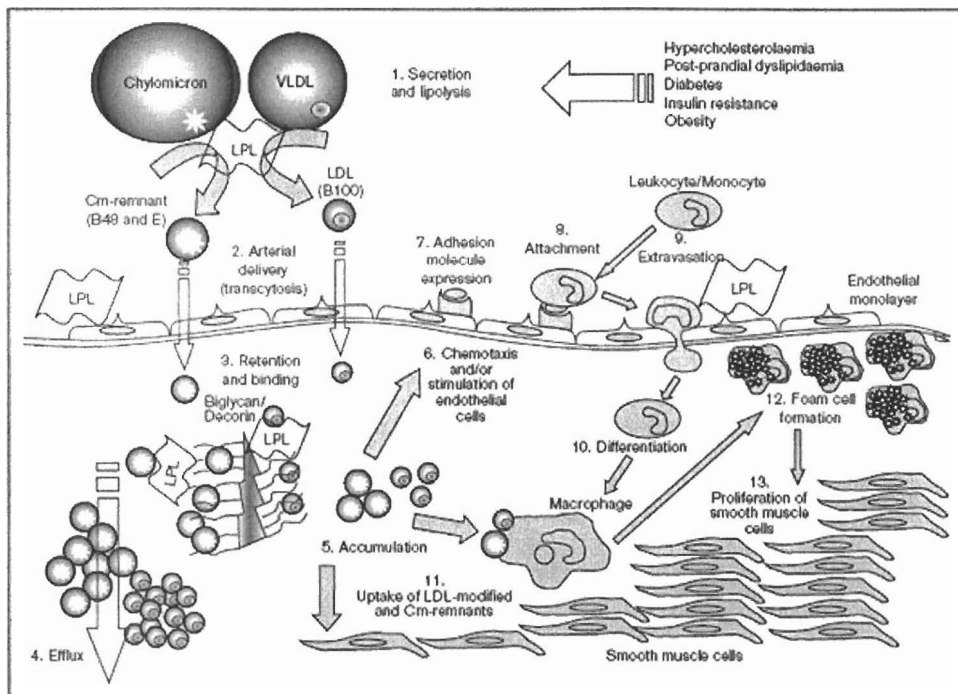
The next major atherosclerosis hypothesis, which has been widely researched and expanded upon, is the oxidative modification hypothesis. This hypothesis was first proposed in 1989 by Steinberg *et al.* and placed more emphasis on the LDL particle itself.<sup>6</sup> The basis of this hypothesis stems from observations that LDL particles in their native state are not atherogenic and LDL particles that are modified chemically are atherogenic by being more susceptible to internalization by macrophages through a “scavenger receptor” pathway.<sup>7</sup> This process begins when LDL crosses into the subendothelial space of a lesion prone area of the artery and becomes exposed to oxidation. Oxidation causes modification of the lysine groups on apo B-100; these modifications in turn cause the LDL particle to become more negatively charged and more susceptible to macrophage internalization. Oxidized LDL particles also stimulate monocyte recruitment into the

intimal space and prevent macrophages already in the intima from leaving. This increases the chances for more LDL to become oxidized and enter the scavenger receptor pathway. Since this is not a regulated pathway, uptake of cholesterol in oxidized LDL is continual and foam cell accumulation and foam cell necrosis occurs.<sup>8</sup> This necrosis results in endothelial dysfunction and injury.<sup>9</sup>

### **1.3 Response-to-Retention Hypothesis**

Finally, Williams and Tabas were the first to pioneer the response-to-retention hypothesis in 1995. They concluded that the key pathogenic event that is “both necessary and sufficient to provoke lesion initiation in a normal artery” is lipoprotein retention.<sup>10</sup> Lipoprotein retention involves several key components which are proteoglycans in the extracellular matrix, lipolytic enzymes such as lipoprotein lipase and sphingomyelinase, possibly other structural elements, and of course, atherogenic lipoproteins namely LDL. Williams and Tabas described a hypothetical pathway of the early stages of atherosclerosis starting with apo B containing lipoproteins entering the extracellular matrix by transcytosis and binding to arterial proteoglycans, which they call retentive molecules. This inward flow of lipoproteins causes LDL accumulation by proteoglycans and LDL aggregation by other arterial components like secretory sphingomyelinase. The accumulation and aggregation of lipoproteins further triggers a proinflammatory cascade that involves chemotaxis, adhesion molecule expression, and monocyte/leukocyte attachment and migration into the intima. Then the monocyte/leukocyte differentiates into a macrophage

which can take up modified LDL in the intima which can lead to foam cell formation and cause smooth muscle cells to proliferate and migrate. (Figure 1)



The present review discusses the initial stages of lipoprotein arterial delivery, retention and efflux (shown as stages 1-5). The accumulation of cholesterol-rich apolipoprotein B (apoB<sub>48</sub>/B<sub>100</sub>)-containing lipoproteins within the arterial wall is thought to further trigger pro-inflammatory cascade (shown as stages 6-13). Cm-remnant, chylomicron remnants; LPL, lipoprotein lipase.

Figure 1 Early stages of atherogenesis. Schematic representation of the Response to Retention Hypothesis. Cm-remnant – chylomicron remnant, LPL – lipoprotein lipase, VLDL – very low-density lipoprotein, LDL – low-density lipoprotein. (Proctor *et al.*)<sup>11</sup>

These hypotheses of atherosclerosis are not mutually exclusive but rather emphasize different concepts as the necessary and sufficient events to support the development of atherosclerotic lesions.<sup>12</sup> A time might come where all these hypotheses will ultimately fit together for a deeper understanding of the atherosclerotic process and it is not just one component that is the absolute critical. Until then, more questions need to be answered. Knowing this, there has been much research done based on the response to retention hypothesis, focusing on the interactions of proteoglycans and low density lipoproteins. In the sections to follow, the functions and structures of proteoglycans and glycosaminoglycans relating to atherosclerosis will be discussed along with a brief background of low density lipoproteins.

#### **1.4 Proteoglycans and Glycosaminoglycans**

Proteoglycans are complex molecules composed of a core protein and many covalently linked negatively charged glycosaminoglycan (GAG) chains.<sup>13, 14</sup> Proteoglycans are generally assembled in the golgi apparatus of a mammalian cell; although, proteoglycans relevant to our discussion are produced in smooth muscle cells along with other components of the extracellular matrix like collagens and elastins. Proteoglycans are a major component found in the intima of large arteries. These molecules form a three-dimensional network that occupies 60% of the intima.<sup>15</sup> There are many types of proteoglycans found in the body that hold different functions, but the proteoglycans that are most abundant in the vascular wall are versican and biglycan/decorin. Versican is a member of the aggrecan family and has a core protein of

~263 KD and 15 to 20 glycosaminoglycan (GAG) chains. It is made of about 70% chondroitin 6-sulphate, 20% chondroitin 4-sulphate (C4S), and 10% dermatan sulphate (DS). Biglycan and decorin are smaller proteoglycans with core proteins of 36-38 KD and 2 to 3 GAG chains of DS or chondroitin sulphate (CS)<sup>16</sup> (Figure 2A). It has been reported by Wasty *et. al.* that the aforementioned CS and DS GAGs of lesion prone regions of human aortas have higher affinity for apo B lipoproteins than GAGs of non-lesion-prone aortic segments.<sup>17</sup> Another GAG that has been associated with apo B binding is heparin.<sup>18</sup>

Chondroitin sulphate and dermatan sulphate are two of the six major glycosaminoglycan chains. Dermatan sulphate is a derivative of chondroitin sulphate (Figure 2B). Glycosaminoglycans are polysaccharides, mainly of repeating disaccharide units. One sugar of the disaccharide is either N-acetylglucosamine or N-acetylgalactosamine and the second is usually either glucuronic acid or iduronic acid.<sup>19</sup> Also, at least one of the sugars in the repeating unit has a negatively charged carboxylate or sulphate group. Chondroitin sulphate, keratan sulphate, heparin, heparan sulphate, dermatan sulphate, and hyaluronate are the major glycosaminoglycans.<sup>20</sup> Glycosaminoglycans are attached to serine residues of the protein core of the proteoglycans through a trisaccharide linker of galactose-galactose-xylose (Figure 3).



A

## Proteoglycans

CS (30-50 Kd)

Core protein  
(260 Kd)



Versican

DS (30-50 Kd)

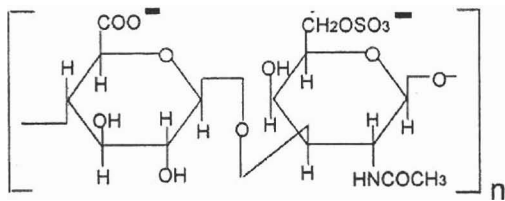
Core Protein  
(40 Kd)

Biglycan

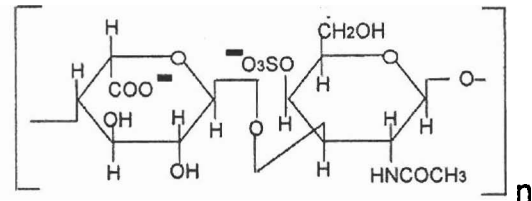


B

## Glycosaminoglycans



Chondroitin 6-sulphate



Dermatan sulphate

Figure 2 Proteoglycans and Glycosaminoglycans. (A) Versican and Biglycan/Decorin, examples of chondroitin sulphate proteoglycans. (B) Fisher diagrams of chondroitin 6-sulphate and dermatan sulphate (derivatives of chondroitin sulphate). Adapted from Camejo *et. al.*<sup>14</sup>

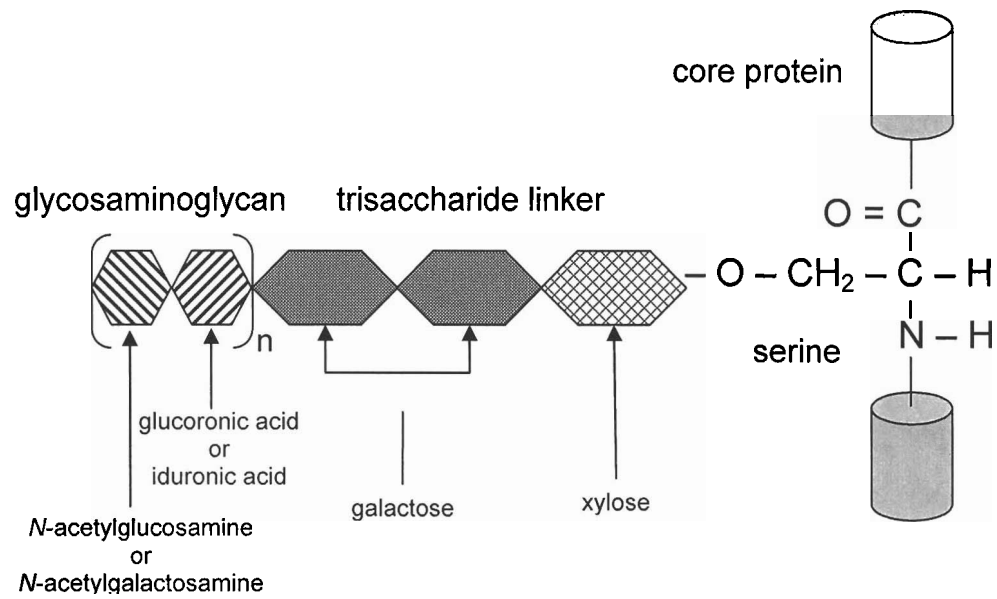


Figure 3 How Glycosaminoglycans Are Linked to the Protein Core of Proteoglycans.  
Adapted from M.W. King.<sup>21</sup>

## 1.5 Lipoprotein Production and Cholesterol Metabolism

Lipids can be produced both exogenously and endogenously.<sup>22</sup> Exogenously, lipids, mainly triglyceride, come from the diet. These dietary lipids are absorbed by the small intestine, metabolized and secreted as chylomicrons. Chylomicrons are very large particles (180 – 500 nm and MW 400,000 KD) and can contain apolipoproteins E, C-II, C-III, A-I, A-II, and B-48. Once in the blood, lipoprotein lipase catabolizes the triglycerides in the chylomicrons to free fatty acids and glycerol. At the same time, there is a transfer of apo C-II, C-III, and E to HDL and a chylomicron remnant is formed. Chylomicron remnants contain one copy of apo B-48 and many copies of apo E. These remnants are then recognized by the liver through the LDL-receptor (apo B/E receptor) and the LDL-receptor related protein (LRP). Apo C-II, C-III, and E that are being carried by HDL get transferred back to chylomicrons still remaining in the blood and the cycle continues.

Endogenously, lipids needed for the formation of lipoproteins are already present in the body. Synthesis and secretion both occur in the liver beginning with very low-density lipoproteins (VLDL).<sup>22</sup> VLDL is a large, triglyceride rich lipoprotein and contains apolipoproteins B100, C, and E. As with the chylomicrons, lipoprotein lipase removes triglycerides along with apo C and phospholipids from VLDL to produce a VLDL remnant called intermediate density lipoproteins (IDL). IDL is converted to LDL by hepatic lipase. Hepatic lipase removes more triglycerides and the remaining apo E and a little more phospholipids creating a cholesteryl ester rich lipoprotein.<sup>23</sup> Most LDL in the body is produced endogenously.

Endogenous production of cholesterol starts when acetyl-CoA from the citric acid cycle is converted to acetoacetyl-CoA by the enzyme thiolase and both the aforementioned substrates are condensed to form 3-hydroxy-3-methylglutaryl-CoA (HMG-CoA). HMG-CoA is then reduced to mevalonate by HMG-CoA reductase and NADPH. This is the first step in the HMG-CoA reductase pathway and the rate limiting step in cholesterol synthesis. (A class of drugs called statins, HMG-CoA reductase inhibitors, specifically targets this enzyme and inhibit cholesterol synthesis.) A long series of reactions produces hydrophobic molecules that are used for different but important tasks, such as, cell membrane maintenance, production of hormones, protein anchoring and *N*-glycosylation.<sup>24</sup> The transcription of the HMG-CoA reductase gene is enhanced by the sterol regulatory element binding protein (SREBP). The inactive form of SREBP is located in the ER. Once cholesterol levels fall SREBP is released from the ER by proteolysis and migrates to the nucleus where it binds to the sterol regulatory element (SRE) and transcription of HMG-CoA reductase begins. When cholesterol levels increase the SREBP is cleaved and degraded and transcription ceases.

## 1.6 Low-Density Lipoproteins

Low density lipoproteins have a density range between 1.019 and 1.063 g/ml and a particle size between 19 and 23 nm. Because of this, LDL is naturally heterogeneous. About 45% of the LDL particle's total weight is composed of a neutral lipid core containing cholesteryl esters and triglycerides. On the surface, the phospholipid monolayer comprises ~20% of the particle's total weight, free unesterified cholesterol

~10%, and apo B-100 the remaining ~25% of the particle's total weight. Apo B-100 is the largest known protein containing 4,536 amino acids with three alternating regions of beta sheets and alpha helices (figure 4). It has a molecular weight of 512,723. LDL is the major cholesterol carrying plasma lipoprotein. The native LDL particle is generally positively charged unless it becomes exposed to oxidation. Once oxidation occurs the particle slowly becomes more negatively charged.

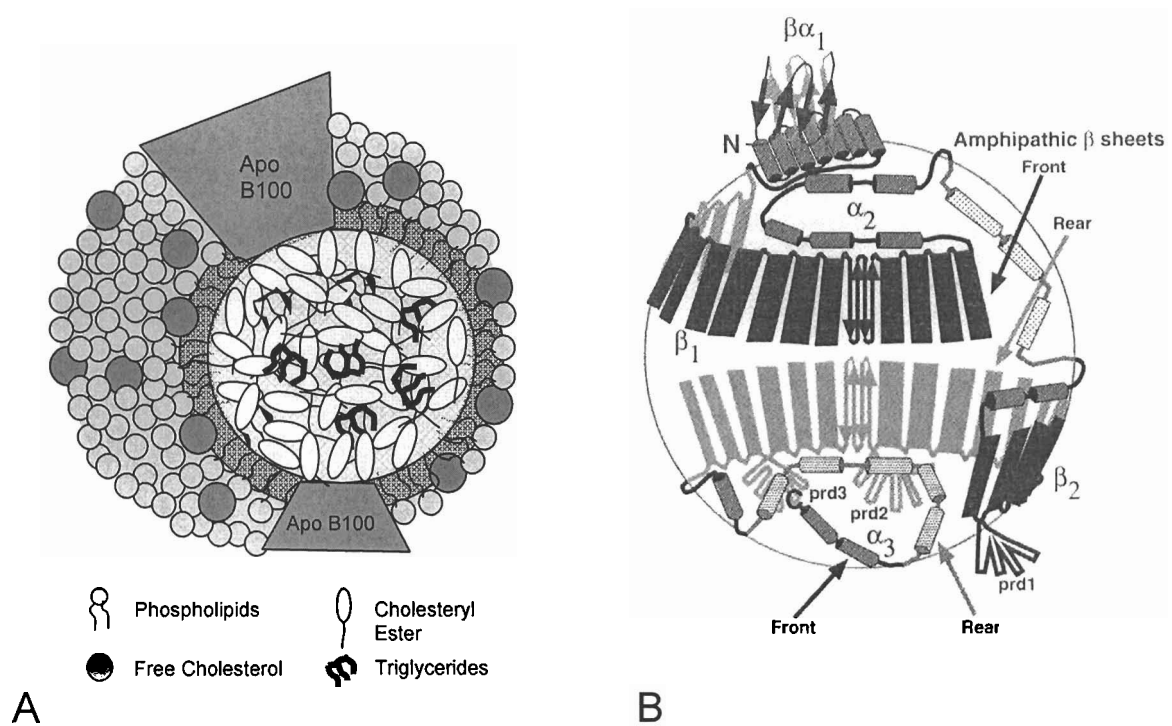


Figure 4 Low-Density Lipoprotein. (A) Schematic representation of an LDL molecule. (B) Schematic representation of the conformation of apo B100. Segrest *et al.* (2001) *J. Lipid Res.* **42**: 1346-1367<sup>25</sup>

### **1.7 LDL's Function in the Body**

In the body, LDL functions as a major contributor in cholesterol metabolism. It is taken into the cell by process called receptor-mediated endocytosis. Apo B-100 on the surface of LDL binds to the LDL receptor, which is localized in a region that contains clathrin coated pits. The LDL and its receptor then become internalized by the clathrin forming a clathrin coated vesicle. Once completely in the cell the clathrin coat depolymerizes into triskelions and the vesicle becomes an early endosome. The early endosome fuses with a late endosome, also known as a sorting endosome, and the LDL separates from the LDL receptor because of the low pH of the environment. The LDL receptor is sent back to the plasma membrane where it is recycled and awaits another LDL particle. In the meantime, the late endosome that contains the LDL fuses with and becomes a lysosome. This is where the apo B-100 is degraded to amino acids and the cholesteryl esters are hydrolyzed into cholesterol and fatty acids. Since the metabolism of cholesterol is part of a negative feedback system, an abundance of cholesterol inhibits the synthesis of more cholesterol and the LDL receptor.<sup>24, 26</sup>

Now that the key players in the atherosclerotic process have been discussed and identified, we can examine the binding properties of low-density lipoproteins with chondroitin 6-sulphate.

### **1.8 Low-Density Lipoprotein – Glycosaminoglycan Interaction**

The present understanding is that the interaction between LDL and the GAG chains on proteoglycans occurs through ionic attraction between positively charged clusters amino

acids on apolipoprotein B-100 and the negatively charged sulphate groups on the GAG chains of proteoglycans.<sup>27</sup> Chondroitin sulphate was chosen for our study because it is the most abundant glycosaminoglycan in the body and the predominant one in atherosclerotic lesions. (Chondroitin 6-sulphate was used specifically over chondroitin 4-sulphate because it is more sterically accessible to LDL complex formation.)

### **1.9 Physical State of the LDL Core**

To assess the physical state of the LDL core, the phase transition temperature was determined by differential scanning calorimetry. Early studies by Deckelbaum *et. al.* characterized the different types of phase transitions of LDL, namely that of a reversible transition. This reversible transition in the LDL core takes place near body temperature and is associated with a liquid crystalline order-disorder phase change of cholesteryl esters.<sup>28</sup> Later, our lab correlated the phase transition of the LDL core with changes in secondary structure of the apo B100. This indicated that the conformation of apo B100 depends on the physical state of the LDL core and less on the composition of the core.<sup>29</sup> Since it has been shown in our lab that LDL samples from different individuals may have different phase transition temperatures the next logical progression in our research was to examine how these individual LDL samples bind to chondroitin 6-sulphate.

### **1.10 Hypothesis**

In the present study, we examined the correlation between the physical state of the LDL core and the ability of the LDL particle to bind to chondroitin 6-sulphate. We



hypothesized that the physical state of the LDL core, through its influence on the conformation of apo B-100<sup>29</sup>, influences the binding of LDL to C6S.

The phase transition temperature of each LDL sample was determined by differential scanning calorimetry. LDL-C6S turbidity binding assays were performed for various LDL samples. Additionally, compositional analyses including assays for protein, total cholesterol, free cholesterol, triglyceride, and phospholipids were completed along with SDS PAGE to verify that apo B-100 was intact.

Our results showed that the physical state of the LDL core does not have any affect on the LDL particle's ability to bind to chondroitin 6-sulphate. However, we found that certain lipids significantly correlated with binding, indicating that large, lipid-rich LDL particles have a higher capacity to bind C6S than smaller, lipid poor LDL.

## CHAPTER 2 MATERIALS AND METHODS

### 2.1 Isolation of Lipoproteins

Lipoproteins were isolated as described by Schumaker and Puppione.<sup>30</sup> Fifty milliliter blood samples were drawn from healthy, normolipidemic individuals after a 12 hour fast. Samples were collected into five 10 ml Beckton Dickinson Vacutainer tubes (BD: Franklin Lakes, NJ) containing EDTA, then transferred into plastic centrifuge tubes and spun at 5,000 rpm for 20 minutes at 4°C using a Sorvall SS-34 rotor (Sorvall: Newtown, CT) in a Sorvall RC-5B refrigerated superspeed centrifuge (Dupont Instruments: Wilmington, DE). Once the blood cells and the plasma separated, the top clear plasma layer was collected and supplemented with 5 mM disodium ethylenediaminetetraacetate (EDTA), 0.02% Sodium Azide ( $\text{NaN}_3$ ), 5  $\mu\text{g/ml}$  gentamycin, 0.2 U/ml aprotinin, and 50  $\mu\text{g/ml}$  leupeptin (Sigma-Aldridge: St. Louis, MO). The densities of the plasma solution and deionized water were adjusted to a density range between 1.019 to 1.21 (depending on which lipoprotein subclass is being separated) with a stock KBr solution and distributed equally into two Beckman ultracentrifuge tubes with the plasma in the bottom of the tube overlaid with the adjusted deionized water. A series of sequential ultracentrifugations were performed using a Beckman Ti70 rotor (Beckman Coulter: Fullerton, CA) to separate very low density lipoprotein (VLDL) and intermediate

density lipoprotein (IDL), low density lipoprotein (LDL), high density lipoprotein (HDL), and lipoprotein deficient plasma (LPDP).<sup>30</sup>

To remove the VLDL/IDL layer, whole plasma and an overlay solution was adjusted to a density of 1.019. The whole plasma was distributed between two Beckman ultracentrifuge tubes (Beckman Coulter: Fullerton, CA), overlayed, balanced and placed in the Beckman Ti70 rotor (Beckman Coulter: Fullerton, CA). The plasma was centrifuged in a Beckman L8M or L7-55 ultracentrifuge (Beckman Coulter: Fullerton, CA) for 19 to 24 hours at 40,000 rpm and 20°C. After 24 hours, the tubes were removed from the rotor and a separated VLDL/IDL top layer could be seen. Using a Pasteur pipette, the top VLDL/IDL layer was removed and properly discarded. The middle layer, which consisted of the overlay solution, was collected for density determination and also properly discarded. The bottom layer, which contains LDL and HDL was collected and used for further lipoprotein separation. The remaining plasma containing LDL and HDL was adjusted to a density of 1.063 and deionized water adjusted to the same density was used as an overlay. As before, the plasma was distributed between two Beckman ultracentrifuge tubes (Beckman Coulter: Fullerton, CA), overlayed, balanced, placed in the rotor and centrifuged for 19 to 24 hours at 40,000 rpm at 20°C. After 24 hours, the tubes were removed from the rotor and an apparent separation of LDL and HDL can be seen. A Pasteur pipette was used to collect the top layer of LDL. The LDL was desalted by an overnight dialysis in PBS containing 150 mM sodium chloride, 10 mM sodium phosphate, 5 mM EDTA, and 0.02% azide and placed in a temperature controlled environment set to 4°C. The middle overlay solution was used for density determination and then properly

discarded. The remaining plasma containing HDL was either separated by another centrifugation step for later use or properly discarded.

After dialysis, LDL was recollected and transferred to an air tight plastic storage tube. The LDL sample was stored under argon at 4°C until further experimentation.

## **2.2 Compositional Analysis**

Protein concentrations were determined by a modified Lowry procedure, using bovine serum albumin as a standard.<sup>31</sup> Total cholesterol, free cholesterol and phospholipids concentrations were determined by using enzymatic assay kits obtained from Wako Chemicals USA, Inc. (Richmond, VA). Cholesteryl ester concentrations were calculated by subtracting free cholesterol from total cholesterol and multiplying the value by 1.68.<sup>32</sup> Triglyceride concentrations were determined by using an enzymatic assay kit obtained from ThermoTrace (Melbourne, Australia). All kit assays were performed using manufacturer's instruction.

## **2.3 Sodium Dodecyl Sulphate Polyacrylamide Gel Electrophoresis (SDS-PAGE)**

SDS PAGE was performed using a procedure from Laemmli.<sup>33</sup> Samples were prepared by adding 1 µl of LDL to 5 µl of deionized water and 10 µl of sample buffer. The sample buffer consisted of 20% glycerol (v/v), 25% Tris buffer (v/v) (1 M Tris, pH 6.8), 2% mercaptoethanol (v/v), 10% SDS (w/v), and 1% Bromophenol Blue by weight. Each loading samples was prepared in a top perforated eppendorf and placed in a water bath and boiled for 5 minutes to denature the proteins. Meanwhile, a Tris-HCl Ready gel

with a 4-15% linear gradient manufactured by Bio-Rad (Hercules, CA) was prepared. The gel was submerged in a Tris Buffer (25 mM Tris, 0.192 M glycine, 3.5 mM SDS in water, pH 8.3) and once loading samples were ready they were loaded into the gel. A prestained broad range standard (BioRad, control 947560) was used as a marker. After standard and samples were loaded, the gel underwent electrophoresis for about 30-45 minutes at 200 volts until the samples ran to the bottom of the gel. Subsequently, the gel was removed from its cartridge and a coomassie stain (1% coomassie blue in 50% methanol, and 10% acetic acid) was applied for at least thirty minutes up to overnight. Subsequently, the gel was destained with a solution of 10% acetic acid, and 15% methanol.<sup>33</sup> The destaining solution was applied for at least 8 hours. Stained gels were digitized using a flat bed scanner and the UMAX MagicScan program (Dallas, Texas).

## **2.4 Differential Scanning Calorimetry (DSC)**

LDL samples were dialyzed in a buffer containing 150 mM sodium chloride and 10 mM sodium phosphate at pH 7.4 (PBS). Three milliliters of the dialysis buffer was collected to serve as the reference for the baseline. LDL samples were diluted to a concentration of 0.7 mg/ml or greater. The reference and the sample were both degassed in a chamber that reached between 25 and 30 psi for 10 minutes. Using a Nano-II Differential Scanning Calorimeter (Calorimetry Science Corporation: American Fork, UT), 600  $\mu$ l of LDL was loaded in a sample compartment and 600  $\mu$ l of PBS was loaded in a reference compartment. A baseline was obtained by loading 600  $\mu$ l of PBS in the sample compartment and 600  $\mu$ l of PBS in the reference compartment. The accompanying

software was programmed to analyze 3 temperature-increasing (up-) scans and 3 temperature-decreasing (down-) scans within the 5°C to 55°C temperature interval. Triple up- and down- scans were performed to demonstrate reversibility and reproducibility of the observed phase transitions. Data analysis was obtained by using CpConvert Software version 2.1.1 (Applied Thermodynamics: Hunt Valley, MD).

## **2.5 Electrophoretic Mobility Shift Gels**

A 0.8% or 1.2% E-gel System precast agarose gel (Invitrogen Corporation: Carlsbad, CA) was used to determine the level of oxidation of the LDL samples in their native state. After preparing a LDL sample concentration of 7 µg/ml, 14 µg/ml Sudan Black was added and PBS at pH 8.6 was added to the reaction volume, totaling 20 µl in each well. The gel was pre-equilibrated without samples for two minutes. After loading the samples, the gel was run for 30-45 minutes at 60V. The gels were digitized using a flat bed scanner and the UMAX MagicScan program (Dallas, TX).

## **2.6 Spectrophotometric Determination of Conjugated Dienes**

Conjugated dienes in an LDL sample were determined using a set protocol in spectrophotometer (Lamda 20 spectrophotometer Perkin Elmer: Norwalk, CT).<sup>34</sup> A 50 µg sample of LDL in 1 ml of PBS (without EDTA and NaN<sub>3</sub>) was prepared in a Fisherbrand\* quartz cuvette (Fisher Scientific International: Pittsburg, PA). Another cuvette containing only PBS without EDTA and NaN<sub>3</sub> served as the blank. The absorbance of the samples

was determined at 234 nm. LDL samples with absorbance in excess of 0.25 were considered oxidized and were not used for further analysis.

## **2.7 LDL-C6S Turbidity Binding Assays**

Turbidity assays were carried out in a binding buffer that contained 2.5 mM Tris, 5 mM CaCl<sub>2</sub>, 1 mM magnesium chloride, and 7.5 mM sodium chloride, pH 6.0, essentially according to Hurt *et. al.*<sup>35</sup> and Mourao *et. al.*<sup>36</sup>. A stock solution of Chondroitin 6-sulphate (Sigma-Aldridge: St. Louis, MO) was made with a concentration of 0.1 mg/ml in the binding buffer. Chondroitin 6-sulphate was used at concentrations of 0.13, 0.25, 0.50, 0.75, 1.00, and 1.25 µg/ml, separately, in each assay. Twenty-five micrograms per milliliter of an individual LDL sample was added to the binding buffer in a methacrylate cuvette (Fisher Scientific International: Pittsburg, PA) and used as a blank for the turbidity assay. Once the blank is recognized, the chondroitin 6-sulphate is added and the assay is incubated for 2 hours at either 37°C or 24°C. The total reaction volume was 1 ml. The turbidity of the solution was measured at 600 nm using a Lamda 20 spectrophotometer (Perkin Elmer: Norwalk, CT). Turbidity assays were completed in triplicate for each individual LDL sample.

## **2.8 Statistical Analysis**

Correlational analyses were performed using GraphPad Prism version 4.00 for Windows (GraphPad Software: San Diego, CA). Graphs with P-values of less than 0.05 were significant. P-values were obtained from GraphPad Prism 4 software.

## **2.9 Nuclear Magnetic Resonance Analysis – LipoScience, Inc.**

LDL size was determined by Nuclear Magnetic Resonance (NMR) Analysis, as described by Otvos *et. al.*<sup>37, 38</sup> One milliliter samples of whole plasma, which contains all the lipoproteins present – VLDL, IDL, LDL, and HDL – were collected in a sample container, frozen at -80°C, shipped to LipoScience, Inc. (Raleigh, NC) for NMR analysis. Typical data output sheets are shown in figures 5 and 6. Only LDL size data of the analyses were used for this study.



## LIPOPROFILE PANEL

### Coronary Heart Disease (CHD) Risk Categories

	nmol/L	Goal for High-Risk Patient	Goal for Moderately High-Risk Patient	Borderline High Risk	High Risk	Very High Risk
<b>LDL Particle Number (LDL-P™)</b>	<b>1024</b>	under 1000	<b>under 1300</b>	1300-1599	1600-2000	over 2000

**For High-Risk Patients with CHD or CHD Risk Equivalents:**  
 -primary goal: LDL-C < 100 mg/dL and LDL-P < 1000 nmol/L  
 -secondary goal: Small LDL particle number < 700 nmol/L (< 50th percentile; see subclass levels graph on page 2)

**For Moderately High-Risk Patients (10-20% 10-year risk):**  
 -primary goal: LDL-C < 130 mg/dL and LDL-P < 1300 nmol/L  
 -secondary goal: Small LDL particle number < 700 nmol/L (< 50th percentile; see subclass levels graph on page 2)

LDL Size	nm	Pattern A (large LDL)		Pattern B (small LDL)	
	21.9	23.0 - 20.6 Lower Risk		20.5 - 18.0 Higher Risk	
Large HDL (cholesterol)	mg/dL	Lower Risk	Intermediate	Higher Risk	
	39	greater than 30	30 - 11	less than 11	
Large VLDL (triglyceride)	mg/dL	Lower Risk	Intermediate	Higher Risk	
	17	less than 7	7 - 27	greater than 27	

LDL Particle Size (small), Large HDL (low levels), and Large VLDL (high levels) contribute to CHD risk and are important markers of the Metabolic Syndrome and risk of developing Type 2 Diabetes Mellitus.

## PRIMARY PREVENTION PANEL

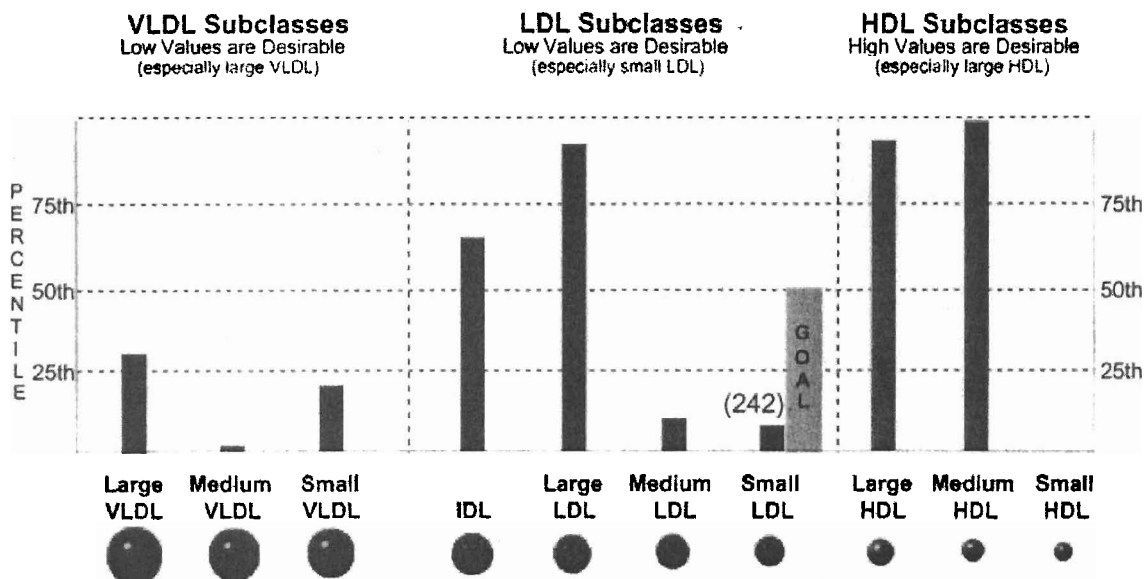
*Elevated numbers of LDL particles and the lipoprotein traits of the metabolic syndrome affect CHD risk interactively. Risk is highest when both are present.*

<b>Elevated LDL Particle Number</b>	<b>&gt;1300 nmol/L</b>	<b>Lipoprotein Traits of the Metabolic Syndrome</b>		
<b>Lipoprotein Traits of the Metabolic Syndrome</b>	<b>≥ 2 traits</b>	<b>Small LDL Pattern B</b> (≤ 20.5 nm)	<b>Reduced Large HDL</b> (< 11 mg/dL)	<b>Elevated Large VLDL</b> (> 27 mg/dL)

*Other identifiers of the metabolic syndrome include abdominal obesity, elevated blood pressure, and fasting glucose ≥ 110 mg/dL.*

Figure 5 NMR LipoProfile® Report (Page 1).

## SUBCLASS LEVELS



Subclass levels are given in percentile units to indicate whether values are high or low, relative to those in a reference population consisting of > 6900 subjects enrolled in the Multi-Ethnic Study of Atherosclerosis (MESA).

The concentration of small LDL particles (in nmol/L) is given in parentheses above the percentile bar. The suggested secondary treatment goal for high-risk and moderately high-risk patients is < 700 nmol/L (< 50th percentile).

## NMR-DERIVED LIPID VALUES

		Current NCEP Risk Categories			
	mg/dL	Desirable	Borderline-High	High	
<b>Total Cholesterol</b>	<b>186</b>	less than 200	200 - 239	240 or greater	
	mg/dL	Optimal	Near or above optimal	Borderline-High	High
<b>LDL Cholesterol</b>	<b>113</b>	under 100	100 - 129	130 - 159	160 - 190
	mg/dL	Negative Risk Factor		Intermediate	Positive Risk Factor
<b>HDL Cholesterol</b>	<b>66</b>	60 or greater		59 - 40	less than 40
	mg/dL	Normal	Borderline-High	High	Very High
<b>Triglycerides</b>	<b>65</b>	less than 150	150 - 199	200 - 500	over 500

*NMR directly measures the VLDL, LDL, and HDL particles that carry cholesterol and triglycerides. Lipid values are derived by assuming the particles contain a normal amount of cholesterol and triglycerides, and therefore may differ from values given by standard laboratory tests.*

Figure 6 NMR LipoProfile® Report (Page 2).

## CHAPTER 3 RESULTS

### 3.1 Physicochemical Characteristics of LDL

A series of procedures were performed to characterize the composition of the various LDL samples. Assays for protein, total cholesterol, free cholesterol, phospholipids, and triglycerides showed that the LDL samples had normal amounts of each lipid. Sodium Dodecyl Sulphate Polyacrylamide Gel Electrophoresis (SDS-PAGE) confirmed that the protein component of LDL (apolipoprotein B-100) was intact for each LDL sample. Measurement of conjugated dienes ensured that none of the LDL samples had oxidized. Differential Scanning Calorimetry (DSC) provided information on the physical state of the LDL core at a given temperature.

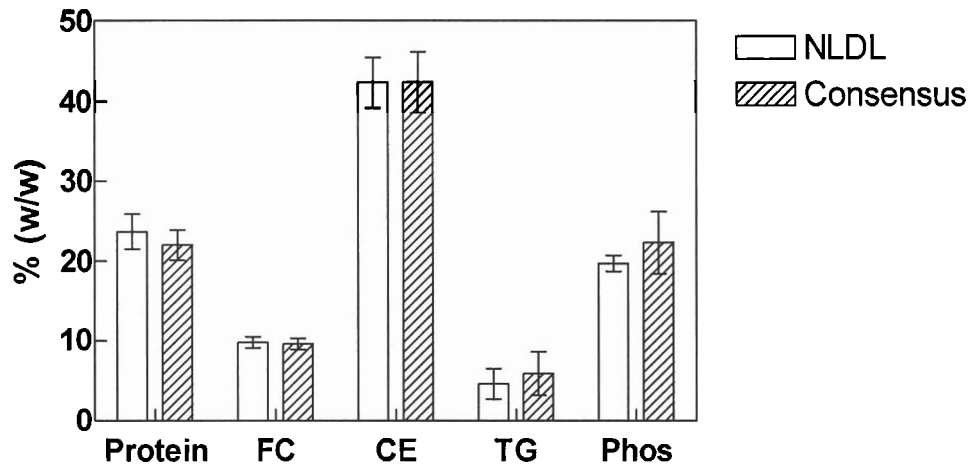
#### 3.1.1 *Lipid Composition*

LDL from 28 healthy normolipidemic subjects were isolated by sequential centrifugation and their physical and chemical properties were analyzed. Assays for protein, total cholesterol, free cholesterol, triglyceride, and phospholipid showed that the LDL samples were compositionally consistent with other published results.<sup>12</sup> Shown in figure 7A, the weight percentage of each lipid component in mean and standard deviation were as follows:  $23.7 \pm 2.2$  for protein,  $9.8 \pm 0.7$  for free cholesterol,  $42.3 \pm 3.1$  for cholesteryl ester,  $4.6 \pm 1.9$  for triglycerides, and  $19.7 \pm 1.0$  for phospholipids. To further confirm that the LDL samples only contained Apo B-100 and that this lipoprotein was

intact, SDS PAGE was performed (figure 7B). If any contaminations were present like apo E (MW 34 kD), additional centrifugation would be completed to re-separate the different lipoproteins.

A

### Compositional Analysis of NLDL



B

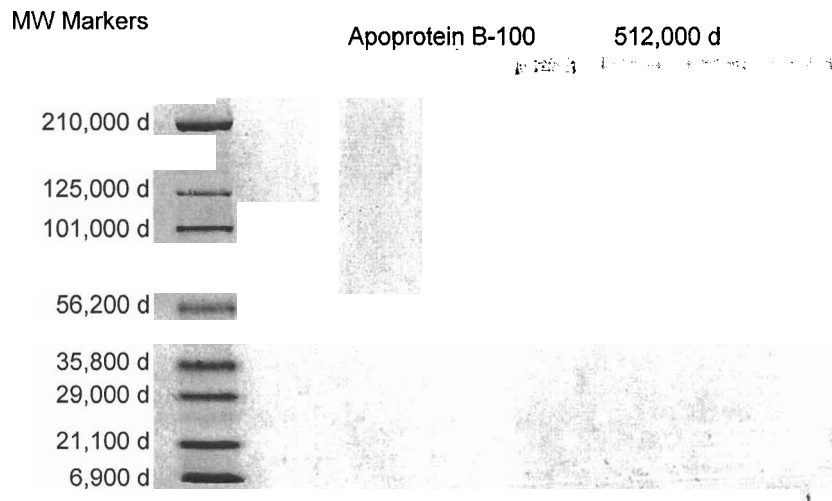


Figure 7 Compositional Analysis LDL. (A) Protein – Apolioprotein B100; FC – Free Cholesterol; CE – Cholesteryl Ester; TG – Triglyceride; Phos - Phospholipid. n=28. Error bars represent  $\pm$ SD. (B) SDS PAGE revealed that all LDL samples were intact forming a band above the first marker which is myosin at 210 kDa. Apo B-100 has a molecular weight of 512,723.

### ***3.1.2 Level of Oxidation***

To provide the best environment for LDL to bind to C6S, one of the main factors is the particle charge and the level of oxidation of an LDL species. LDL is naturally a positively charged particle and C6S is a very negatively charged sugar, their fundamental attraction becomes obvious. Since LDL can be exposed to oxidation, the level of oxidation of the particle becomes important. Before performing C6S turbidity assays, each LDL sample has been supplemented with EDTA and  $\text{NaN}_3$  and assayed very soon after its isolation. To verify the absence of oxidation, the amount of conjugated dienes were detected at an absorbance of 234 nm. Only samples with detection values less than 0.25 were considered not oxidized and used for further experimentation. (Data not shown).

### ***3.1.3 Phase Transition Temperature of LDL***

By determining the phase transition temperature of an LDL sample, it gives information about the physical state of the LDL core, whether it is liquid or liquid crystalline and possible conformation of apo B-100, at physiological temperature 37°C. Figure 8A represents a typical DSC output scan of an individual LDL sample. The area where the curve reaches its peak provides the phase transition temperature of this sample. In this example, the phase transition temperature is 27.5°C. The phase transition temperatures of 20 LDL samples from different individuals were determined. Figure 8B shows the range and variation of phase transition temperatures of a population of healthy individuals. The phase transition temperatures ranged from 22.0°C to 33.8°C. DSC was done in triplicate for each LDL sample, 3 up scans and 3 down scans.

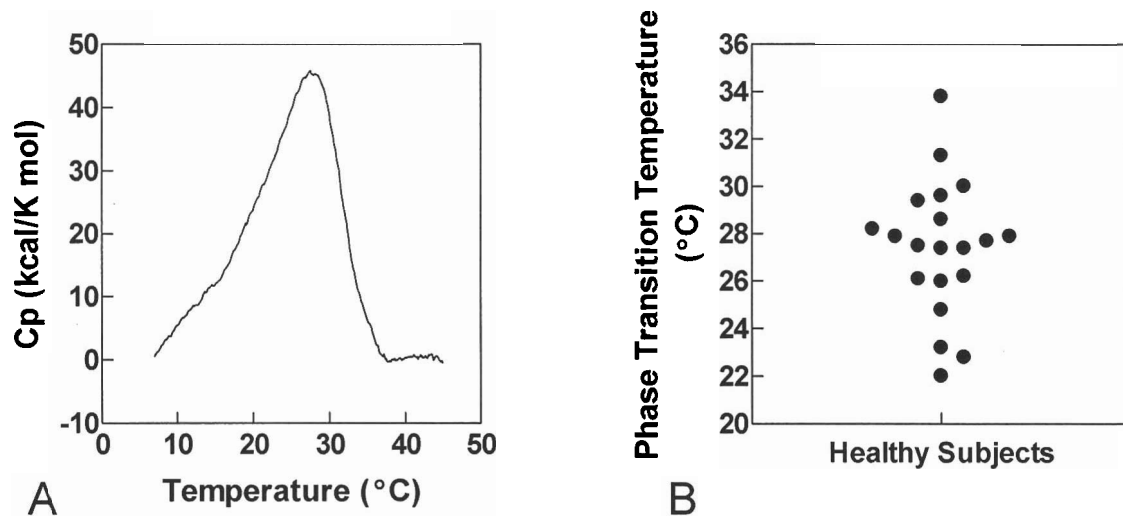


Figure 8 Phase Transition Temperatures. (A) Typical DSC scan. At least 0.5 mg/ml of apo B-100 protein dialyzed in PBS without EDTA and  $\text{NaN}_3$  are loaded into an N-DCS-II Differential Scanning Calorimeter. PBS without EDTA and  $\text{NaN}_3$  are loaded in the reference cell. The temperature range was set for 5°C to 55°C. Samples were run in triplicate – 3 up scans and 3 down scans. (B) Phase transition temperatures taken from 20 LDL samples, determined by differential scanning calorimetry.

### 3.2 LDL:C6S Complex Formation

Turbidity assays were performed to determine binding capacities of 28 different individual LDL samples to chondroitin 6-sulphate. For each LDL sample, turbidity assays were completed in triplicate with the average value used for data analysis. Preliminary studies were done to determine equilibration time and saturation.

Figure 9A is a typical time drive experiment. This time drive experiment measures how turbid the reaction volume becomes over time. The turbidity is caused by the cross linking of the C6S with the LDL in the presence of the binding buffer. 25  $\mu\text{g/ml}$  of apo B protein from each LDL sample was incubated with varying concentrations of chondroitin 6-sulphate, between 0.13  $\mu\text{g/ml}$  – 1.25  $\mu\text{g/ml}$  in binding buffer. At each of the different C6S concentrations the time at which the reaction had reached equilibrium appeared to do so at about two hours. The lowest absorbance reading was observed when the lowest amount of C6S, 0.13  $\mu\text{g/ml}$ , was used in the turbidity assay. The absorbance gradually increased when 0.25, 0.50, and 0.75  $\mu\text{g/ml}$  of C6S was added (in separate assays) and peaked and leveled off with 1.00 and 1.25  $\mu\text{g/ml}$  of C6S. After the 2 hour equilibration period, when all binding sites are occupied, saturation occurs. All experiments were performed in a temperature controlled environment at 37°C. Figure 9B represents the maximum absorbance values of the increasing amounts of C6S. It also shows how two different individuals can have different levels of binding to C6S. In figure 9C, each dot represents an individual LDL sample taken from different healthy individuals. Similar to figure 8B (Phase Transition Temperature versus Healthy Subjects), this shows that in a



population of healthy individuals the level of LDL:C6S binding can vary over a 5-fold range.

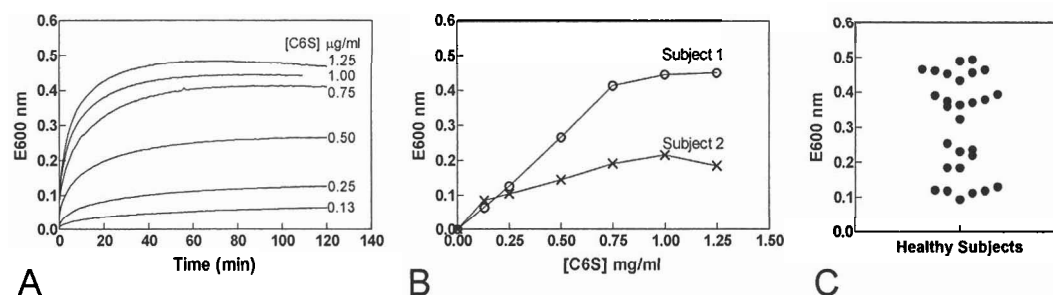


Figure 9 Chondroitin 6-Sulphate Turbidity Assays. (A) Typical Time Drive Experiment with Increasing C6S concentration. 25  $\mu\text{g/ml}$  of an LDL sample was incubated with varying concentrations of chondroitin 6-sulphate, between 0.13  $\mu\text{g/ml}$  – 1.25  $\mu\text{g/ml}$  in a binding buffer of 5mM  $\text{CaCl}_2$ , 2.5mM Tris, 1.0mM  $\text{MgCl}_2$ , and 7.5mM NaCl. Incubations were completed to equilibration after 2 hours at 37°C. (B) Maximal Binding Capacity of 2 Different Individuals. Experiments were carried as previously stated. Maximal binding values were plotted against increasing C6S concentrations. (C) 28 LDL samples underwent C6S turbidity assays. Each assay was performed in triplicate with 25  $\mu\text{g/ml}$  LDL, 1.25  $\mu\text{g/ml}$  C6S, and binding buffer for 2 hours at 37°C.

To measure the amount of apo B-100 that aggregated with C6S, protein assays were completed for a sample that exhibited a higher absorbance value and a sample that had a much lower absorbance value. These same samples were incubated in one set of experiments with varying LDL concentrations and constant C6S concentrations and a second set with varying C6S concentrations with constant LDL concentrations. Figure 10 shows the results of this experiment. When binding experiments were completed for each of these conditions, the reaction mixtures were centrifuged and the pellets were isolated and resuspended for apo B protein determination. It is concluded from this set of data that a “high” binding LDL sample was binding more LDL particles to C6S and that the “low” binding LDL sample was binding fewer LDL particles. A “high” binder is an LDL sample with absorbance detection (E600 nm) of 0.4500 or more. A “low” binder is an LDL sample with absorbance detection (E600 nm) of 0.2500 or less. Similar results were apparent in both experimental conditions.

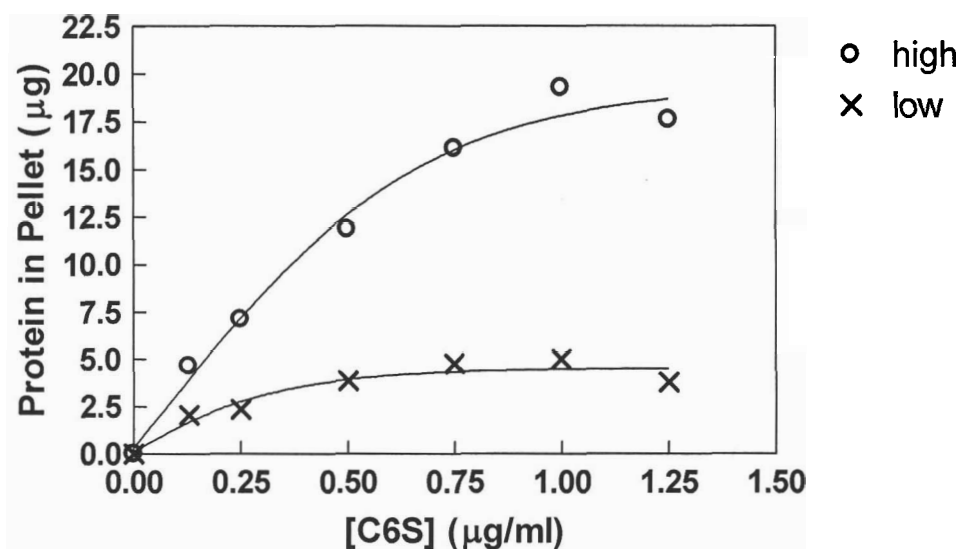
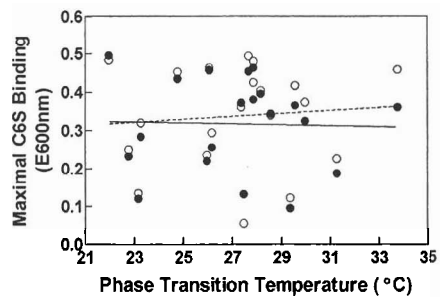


Figure 10 Particle Number versus Aggregation Size. C6S Turbidity Assay Using Varying C6S Concentrations. C6S assays were performed with constant LDL concentration of 25 µg/ml and varying concentrations of C6S ranging from 0.13 µg/ml to 1.25 µg/ml. All assays were completed after 2 hours at 37°C. After 2 hours the reaction mixtures were centrifuged and pellets were formed. Protein concentrations of the pellets were determined.

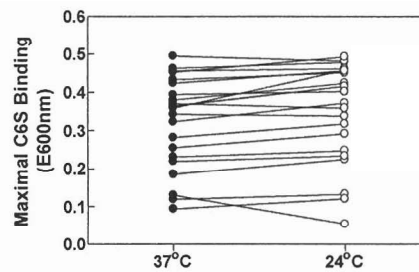
### 3.3 Phase Transition Temperature of the LDL Core and C6S Binding

The phase transition temperatures of 20 different LDL samples were determined by differential scanning calorimetry. The phase transition temperature provides information on the fluidity of the LDL core at a given temperature. These same LDL samples underwent C6S turbidity assays at 37°C and 24°C. Our original hypothesis suggested that the physical state of the LDL core, being liquid or liquid crystalline, affects the binding of the LDL particle to chondroitin 6-sulphate.

The level of aggregation of LDL and C6S glycosaminoglycan chains was measured at an absorbance wavelength of 600 nm. As previously shown, in an isolated population of healthy individuals, they exhibit a range of phase transition temperatures and a range of LDL:C6S aggregation. As shown in figure 11A, turbidity (absorbance at 600 nm) and phase transition temperature did not correlate ( $P < 0.05$ ). Figure 11B pairs each sample at 37°C (when the core is in the liquid state) and 24°C (when the core is in the liquid-crystalline state). When both pieces of information are plotted together, the results disproved our initial assumption; the physical state of the LDL core does not correlate with the level of binding of LDL to C6S.



A



B

Figure 11 Maximal Binding of LDL to C6S. (A) versus Phase Transition Temperature. C6S turbidity assays were performed as mentioned. Assays used 25  $\mu\text{g/ml}$  of LDL and 1.25  $\mu\text{g/ml}$  of C6S for 2 hours and separately at 24°C and 37°C. Absorbance was determined spectrophotometrically at 600 nm. (B) versus Incubations at 37°C and 24°C.

### 3.4 LDL Lipid Composition and C6S Binding

Since no correlation was found between the fluidity of the LDL core and the binding of the LDL particle to C6S. Other factors contributing to C6S binding have to be explored. The specific factors that were chosen to provide additional information on C6S binding were the individual lipid compositions of each LDL preparations. Leading up to our next hypothesis that the lipid composition of the LDL particle contributes to the binding of the LDL particle to chondroitin 6-sulphate.

As previously mentioned, the fluidity of the LDL core determined by the phase transition temperature is caused by the arrangement of cholesteryl esters and triglycerides. To determine if these components had any direct relationship to LDL binding to C6S, a series of compositional correlations were proposed. Figure 12 shows the individual lipid components (figures 12A, 12B, 12D, and 12E) as well as the combination of surface lipids and core lipids (figure 12C and 12F, respectively). Separately, the amounts of phospholipids, free cholesterol, and cholesteryl esters showed significant correlations with the level of binding of LDL to C6S. All of these graphs show a positive correlation for greater binding as phospholipids ( $P < 0.0001$ ,  $r^2 = 0.4591$ ), free cholesterol ( $P < 0.01$ ,  $r^2 = 0.2495$ ), or cholesteryl esters ( $P < 0.005$ ,  $r^2 = 0.2952$ ) increase. Triglycerides showed no significant correlation with binding ( $P > 0.5$ ,  $r^2 = 0.01709$ ). When phospholipids were combined with free cholesterol, as they are naturally as surface lipids, the correlation remained positive and significant ( $P < 0.0005$ ,  $r^2 = 0.4172$ ). Also when the cholesteryl esters and triglycerides were combined, as they naturally are as core lipids, their correlation became better than cholesteryl esters alone. The correlation of the core lipids

and C6S binding became positive and significant ( $P < 0.0005$ ,  $r^2 = 0.4282$ ) even though triglycerides only showed no correlation with binding.



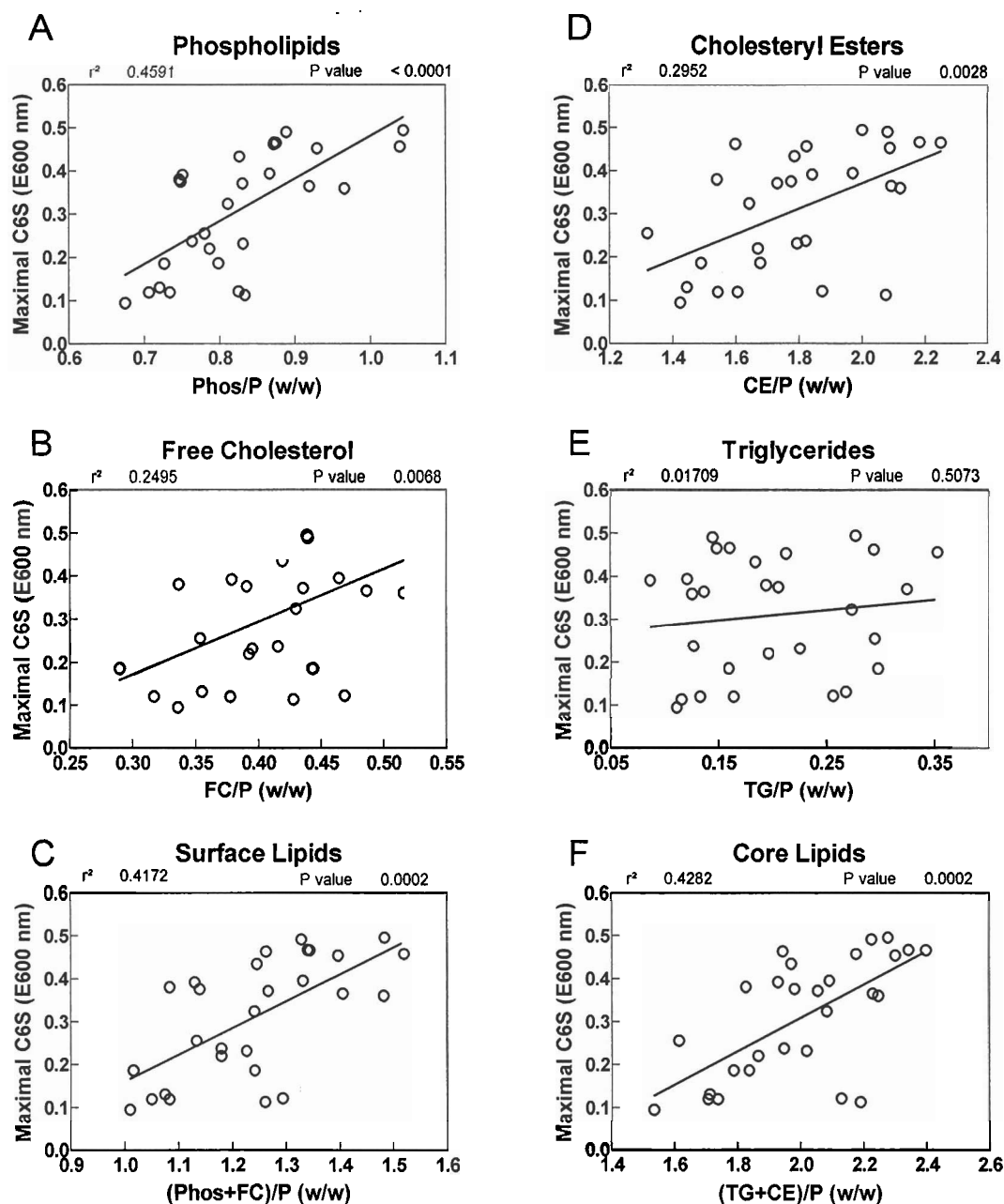


Figure 12 Maximal Binding of LDL to C6S versus Lipid Composition. Each open circle represents an individual LDL sample. Assays for protein, phospholipid, free cholesterol, total cholesterol, and triglycerides were performed. Values were calculated as a weight to weight ratio (w/w), lipid per protein. Cholesteryl esters were calculated by subtracting free cholesterol from total cholesterol and multiplying that value by 1.68.<sup>32</sup> Surface lipids were calculated as phospholipids and free cholesterol per protein. Core lipids were calculated as cholesteryl esters and triglycerides per protein.

Next, we used the same compositional data as previously mentioned and plotted it against 20 LDL samples that had known particle sizes to observe any significant correlations. Figure 13 illustrates the results. Again, phospholipids exhibited a stronger correlation with particle size ( $P < 0.05$ ,  $r^2 = 0.2905$ , figure 13A) than any of the other individual lipid components. Free cholesterol and cholesteryl esters were also both significantly correlated with particle size ( $P < 0.05$ ,  $r^2 = 0.2028$ , figure 13B;  $P < 0.05$ ,  $r^2 = 0.2772$ , figure 13D; respectively) and triglycerides, as before in C6S binding (figure 12D), did not correlated with particle size ( $P = 0.5$ ,  $r^2 = 0.02576$ , figure 13D). When compositional data for phospholipids and free cholesterol were combined, as they are as surface lipids, the correlation improved ( $P < 0.01$ ,  $r^2 = 0.3151$ , figure 13C). Also, when cholesteryl esters were combined with triglycerides, as they are as core lipids, the correlation became significant ( $P < 0.05$ ,  $r^2 = 0.2019$ ).

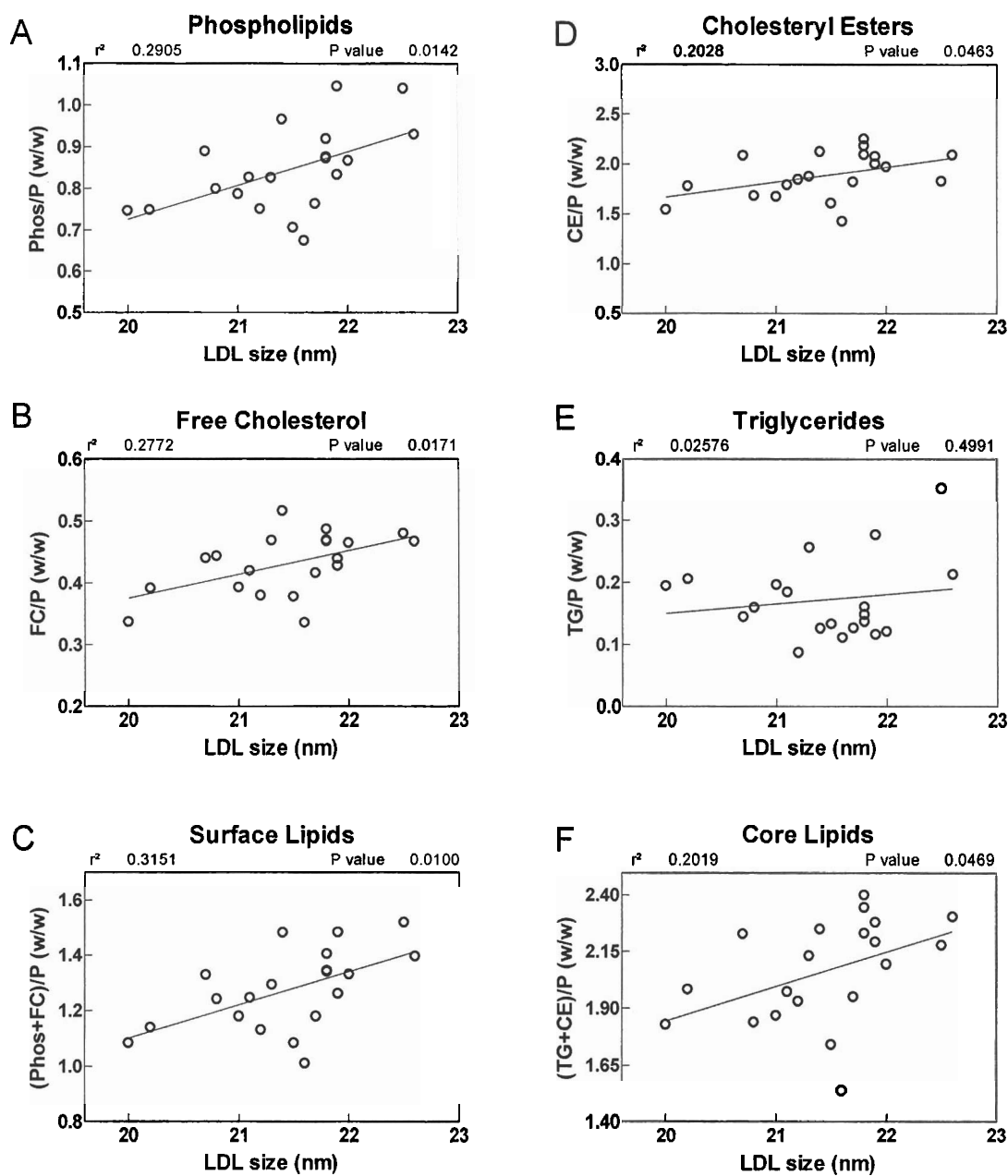


Figure 13 Lipid Composition versus Particle Size. The same data from compositional assays were used as before. Particle size was provided by Liposcience, Inc.  $n = 20$ .

Finally combining the total lipid content (phospholipids, free cholesterol, cholesteryl esters, and triglycerides divided by protein content) and comparing that with the maximal binding gives a strong correlation (figure 14A,  $P < 0.0001$ ,  $r^2 = 0.4538$ ). All of the graphs presented in figure 12 and figure 14 (except figure 14C) provide a strong indication that a larger LDL particle binds better to C6S than a smaller particle. To confirm this assumption, two more correlations were addressed – total lipid content versus LDL particle size and maximal binding of LDL to C6S versus LDL particle size. First, the value for total lipid content was used as above and plotted against LDL size (nm) derived from NMR analysis. Figure 14B demonstrates that more total lipids per particle does positively correlate with a larger particle size ( $P < 0.05$ ,  $r^2 = 0.2619$ ). However, when the level of binding of LDL to C6S was compared with LDL particle size, no significant correlation was found (figure 14C).

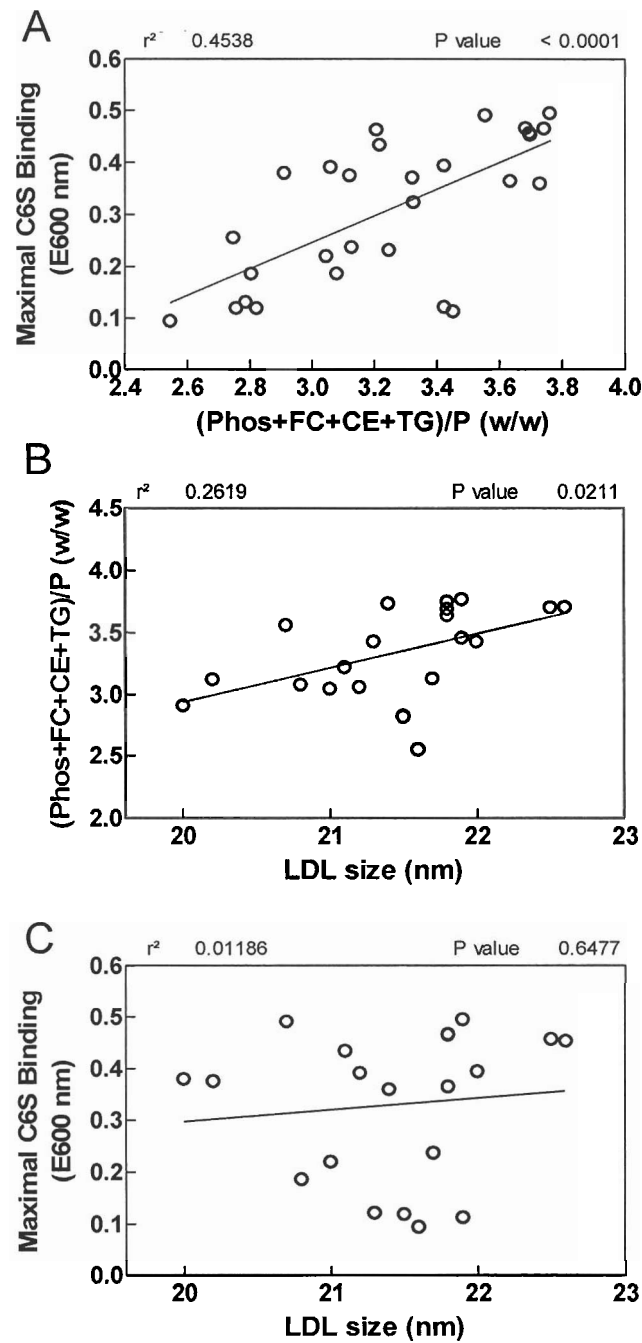


Figure 14 Maximal C6S Binding, Lipid Content, and LDL. Each open circle represents an individual LDL sample. Each assay was completed with 25  $\mu\text{g/ml}$  of LDL and 1.25  $\mu\text{g/ml}$  of C6S. (A) Maximal C6S Binding versus Lipid Content per Protein.  $n=28$ . (B) Total Lipid Content per Protein versus Particle Size.  $n=20$ . (C) Maximal C6S Binding versus Particle Size.  $n=20$ .

## CHAPTER 4 DISCUSSION

In the present study, we investigated the interactions of a variety of LDL samples and their binding properties to purified chondroitin 6-sulphate. The physical state of the LDL core was of particular interest because of its relationship with the conformation of apo B100.<sup>29</sup> The fluidity of the LDL core was determined by its phase transition temperature. Our results illustrated that the physical state of the core does not indicate a strong correlation to the level of binding of the LDL particle to chondroitin 6-sulphate. However, results pertaining to our second hypothesis demonstrate that the LDL composition is directly related to the binding of the LDL particle to chondroitin 6-sulphate. The amount of phospholipids, specifically, shows the best correlation to the LDL particle binding to C6S.

### 4.1 Particle Size: Small versus Large

Not much is mentioned in the literature about LDL lipid composition and its relationship with the interaction between LDL and proteoglycans or glycosaminoglycans. Our results show that the strongest correlation between LDL and C6S binding is with LDL phospholipid content ( $P < 0.0001$ ,  $r^2 = 0.4591$ ) as presented in figure 12A. Phospholipids are found on the LDL particle as surface monolayer lipids. Also, when the amount of phospholipids per LDL particle of each individual sample was analyzed with particle size, it gave the strongest correlation above any of the other lipid components ( $P < 0.05$ ,  $r^2 =$

0.2905 figure 13A). Studies have associated both extremes of subclasses, the larger buoyant<sup>39, 40</sup> and smaller denser<sup>41</sup> LDL subfractions interacting better with arterial proteoglycans.

In a recent review Lada and Rudel, explored the relationship of LDL size, small dense LDL versus large buoyant LDL, and its level of atherogenicity.<sup>42</sup> Small dense LDL has received much notoriety as being the more atherogenic LDL subclass.<sup>43,44,45,46</sup> Possible mechanisms linking small dense LDL as more atherogenic includes it's altered apo B conformation which causes a lowered affinity for the LDL-receptor resulting in longer residence time in the circulation,<sup>43, 44</sup> increased susceptibility to oxidation,<sup>47</sup> increased interaction with the scavenger receptor,<sup>45</sup> and it's ability to easily enter the arterial wall because of its smaller LDL particle size.<sup>46</sup> Another feature of small dense LDL is that it contains little or no sialic acid.<sup>48</sup> Sialic acid may contribute to the size, density,<sup>49</sup> and charge of the LDL particle.<sup>50, 51</sup> Another major factor that places small dense LDL under the spotlight is its role in the metabolic syndrome. The metabolic syndrome is typically associated with elevated triglyceride levels, low HDL levels and a predominance of small dense LDL. Because of this association, research has found that the correlation between small dense LDL as risk factor for CHD also finds high levels of triglycerides and low levels of HDL.<sup>52</sup> As a result, small dense LDL has yet to become an independent risk factor for cardiovascular diseases.

On the other hand, there has been growing evidence that large LDL may be the more atherogenic subfraction. Campos and co-workers<sup>39, 40</sup> have found that in a normolipidemic population with coronary artery disease, large LDL was associated with

increased VLDL and reduced HDL<sub>2</sub> cholesterol levels. Interestingly, after they made adjustments for low HDL cholesterol, high VLDL cholesterol, age, and BMI, large LDL was still an independent risk factor for CAD.<sup>39, 40</sup> It has been shown that large LDL also has low affinity for the LDL receptor, as does small dense LDL, resulting in a longer residence time in the blood.<sup>44</sup> Further studies in nonhuman primates also indicated that large LDL particles contain high amounts of cholesteryl esters in the liquid crystalline state at body temperature, they deliver more cholesteryl ester per particle to cells in the arterial wall, and are associated with increased plaque formation.<sup>53, 54</sup>

## 4.2 Arterial Proteoglycans versus Purified Glycosaminoglycans

Numerous studies have been done on the binding of arterial proteoglycans to LDL but very few on purified glycosaminoglycans. The most studied proteoglycans are ones that consist primarily of chondroitin sulphate. As described in the introduction, proteoglycans consist of various numbers and combinations of glycosaminoglycans attached to a core protein. For example, Anber *et al.*<sup>41</sup> used arterial proteoglycan pools, separated by density, containing a core protein and various amounts of chondroitin sulphate, dermatan sulphate, keratan sulphate, hyaluronic acid. They used a standard solution of arterial proteoglycans that contained 25 µg/ml of chondroitin sulphate in a binding buffer.<sup>44</sup> In our experiments purified chondroitin 6-sulphate glycosaminoglycan was used. It has been suggested that positively charged amino acid clusters on apo B100 are attracted to the highly negatively charged glycosaminoglycans from proteoglycans.<sup>27</sup> Steele *et al.* have confirmed that LDL particles do not bind to the core protein.<sup>55</sup> Further



studies in proteoglycans-LDL binding have shown that the extent of binding is dependent upon the amount of LDL, the concentration of proteoglycans,<sup>56</sup> the degree of glycosaminoglycan sulfation,<sup>57</sup> glycosaminoglycan chain length, and possibly the sites of sulfation.<sup>56</sup> Ballinger *et al.* have suggested that chondroitin 6-sulphate is more sterically accessible to a positively charged apo B100 than chondroitin 4-sulphate which is a more rigid molecule.<sup>56</sup> Differences may also arise in the origin of proteoglycans. For example, proteoglycans produced by smooth muscle cells (in the presence of transforming growth factor beta 1<sup>58</sup>) have different binding properties than proteoglycans secreted by macrophages.<sup>59</sup> As described above, multiple factors affect the binding properties of proteoglycans. In our experiments, we examined only one glycosaminoglycan, the most abundant in the arterial wall, chondroitin 6-sulphate. In using only chondroitin 6-sulphate at constant concentrations, we were able to attribute any changes in binding to the LDL particles of the different individual samples.

Content determines size, so it would be reasonable to assume that, since LDL lipid content is related to LDL-C6S binding then LDL size is related to C6S binding. But, as indicated by our results, LDL size does not appear to correlate with C6S binding. How could that be? Compositional results coincided with other previously published data; however, size data that was used was not the most accurate determination for this study. Because LDL is naturally heterogeneous, the size that was determined by LipoScience was that of an average population size for an individual sample. Therefore the size value that is given is a single value representation of all the different subclass sizes within an individual sample.

Recommended future experimentation could include lipid composition determination after turbidity assay, more importantly, phospholipid concentration. Determining the lipid composition of the LDL particles that have attached to the chondroitin 6-sulfate can provide information about the subclass particularly involved. Another alternative experimental step could be to perform separation of LDL subclasses by density gradient ultracentrifugation. This can possibly indicate which subclasses bind more and which ones bind the least.

At this point, the best indicator for LDL-C6S binding is phospholipid content. Since size data was determined as an average size in a population of LDL particles of an individual LDL sample, the LDL samples may contain varying percentages of LDL subclasses. But, since size had not correlated with chondroitin 6-sulphate binding and correlated instead with lipid content, then that provides more evidence that size is not a good indicator for atherogenicity.

### List of References

### List of References

- 
- <sup>1</sup> Linsel-Nitschke P, Tall AR: **HDL as a target in the treatment of atherosclerotic cardiovascular disease.** *Nat Rev Drug Discov* 2005, **4**(3):193-205.
  - <sup>2</sup> Napoli C, D'Armiento FP, Mancini FP, Postiglione A, Witztum JL, Palumbo G, Palinski W: **Fatty streak formation occurs in human fetal aortas and is greatly enhanced by maternal hypercholesterolemia. Intimal accumulation of low density lipoprotein and its oxidation precede monocyte recruitment into early atherosclerotic lesions.** *J Clin Invest* 1997, **100**(11):2680-2690.
  - <sup>3</sup> Ross R, Glomset JA: **Atherosclerosis and the arterial smooth muscle cell: Proliferation of smooth muscle is a key event in the genesis of the lesions of atherosclerosis.** *Science* 1973, **180**(93):1332-1339.
  - <sup>4</sup> Genes and Disease. Bethesda (MD): National Library of Medicine (US), NCBI.
  - <sup>5</sup> Ross R: **Atherosclerosis is an inflammatory disease.** *Am Heart J* 1999, **138**(5 Pt 2):S419-420.
  - <sup>6</sup> Steinberg D, Parthasarathy S, Carew TE, Khoo JC, Witztum JL. **Beyond cholesterol. Modifications of low-density lipoprotein that increase its atherogenicity.** *N Engl J Med* 1989;**320**(14):915-24.
  - <sup>7</sup> Goldstein JL, Ho YK, Basu SK, Brown MS. **Binding site on macrophages that mediates uptake and degradation of acetylated low density lipoprotein, producing massive cholesterol deposition.** *Proc Natl Acad Sci U S A* 1979;**76**(1):333-7.
  - <sup>8</sup> Ross R. **Atherosclerosis--an inflammatory disease.** *N Engl J Med* 1999;**340**(2):115-26.
  - <sup>9</sup> Quinn MT, Parthasarathy S, Steinberg D. **Endothelial cell-derived chemotactic activity for mouse peritoneal macrophages and the effects of modified forms of low density lipoprotein.** *Proc Natl Acad Sci U S A* 1985;**82**(17):5949-53.
  - <sup>10</sup> Williams KJ, Tabas I. **The response-to-retention hypothesis of early atherogenesis.** *Arterioscler Thromb Vasc Biol* 1995;**15**(5):551-61.

- 
- <sup>11</sup> Proctor SD, Vine DF, Mamo JC. **Arterial retention of apolipoprotein B(48)- and B(100)-containing lipoproteins in atherogenesis.** *Curr Opin Lipidol* 2002;**13**(5):461-70.
- <sup>12</sup> Stocker R, Keaney JF, Jr. **Role of oxidative modifications in atherosclerosis.** *Physiol Rev* 2004;**84**(4):1381-478.
- <sup>13</sup> Rosenberg RD, Shworak NW, Liu J, Schwartz JJ, Zhang L. **Heparan sulphate proteoglycans of the cardiovascular system. Specific structures emerge but how is synthesis regulated?** *J Clin Invest* 1997;**100**(11 Suppl):S67-75.
- <sup>14</sup> Camejo G, Olofsson SO, Lopez F, Carlsson P, Bondjers G. **Identification of Apo B-100 segments mediating the interaction of low density lipoproteins with arterial proteoglycans.** *Arteriosclerosis* 1988;**8**(4):368-77.
- <sup>15</sup> Stary HC, Blankenhorn DH, Chandler AB, Glagov S, Insull W, Jr., Richardson M, Rosenfeld ME, Schaffer SA, Schwartz CJ, Wagner WD and others. **A definition of the intima of human arteries and of its atherosclerosis-prone regions.** A report from the Committee on Vascular Lesions of the Council on Arteriosclerosis, American Heart Association. *Arterioscler Thromb* 1992;**12**(1):120-34.
- <sup>16</sup> Wight TN. **The extracellular matrix and atherosclerosis.** *Curr Opin Lipidol* 1995;**6**(5):326-34.
- <sup>17</sup> Wasty F, Alavi MZ, Moore S. **Distribution of glycosaminoglycans in the intima of human aortas: changes in atherosclerosis and diabetes mellitus.** *Diabetologia* 1993;**36**(4):316-22.
- <sup>18</sup> Olsson U, Ostergren-Lunden G, Moses J. **Glycosaminoglycan-lipoprotein interaction.** *Glycoconj J* 2001;**18**(10):789-97.
- <sup>19</sup> Cooper, Geoffrey M, editor. *The Cell – A Molecular Approach*. 2<sup>nd</sup> ed. Sunderland (MA): Sinauer Associates, Inc; c2000.
- <sup>20</sup> Camejo G. **The interaction of lipids and lipoproteins with the intercellular matrix of arterial tissue: its possible role in atherogenesis.** *Adv Lipid Res* 1982;**19**:1-53.
- <sup>21</sup> <http://web.indstate.edu/thcme/mwking/glycans.html>
- <sup>22</sup> Gotto AM, Jr., Pownall HJ, Havel RJ. **Introduction to the plasma lipoproteins.** *Methods Enzymol* 1986;**128**:3-41.

- 
- <sup>23</sup> Zambon A, Bertocco S, Vitturi N, Polentarutti V, Vianello D, Crepaldi G: **Relevance of hepatic lipase to the metabolism of triacylglycerol-rich lipoproteins.** *Biochem Soc Trans* 2003, **31**(Pt 5):1070-1074.
- <sup>24</sup> Berg JM, Tymoczko JL, Stryer L, editors. *Biochemistry*. New York: W. H. Freeman and Co.; 2002.
- <sup>25</sup> Segrest JP, Jones MK, De Loof H, Dashti N: **Structure of apolipoprotein B-100 in low density lipoproteins.** *J Lipid Res* 2001, **42**(9):1346-1367.
- <sup>26</sup> Lodish H, Berk A, Zipursky SL, Matsudaira P, Baltimore D, Darnell JE, editors. *Molecular Cell Biology*. 4th ed. New York: W. H. Freeman & Co.; c2000.
- <sup>27</sup> Iverius PH. **The interaction between human plasma lipoproteins and connective tissue glycosaminoglycans.** *J Biol Chem* 1972;**247**(8):2607-13.
- <sup>28</sup> Deckelbaum RJ, Shipley GG, Small DM. **Structure and interactions of lipids in human plasma low density lipoproteins.** *J Biol Chem* 1977;**252**(2):744-54.
- <sup>29</sup> Coronado-Gray A, van Antwerpen R. **The physical state of the LDL core influences the conformation of apolipoprotein B-100 on the lipoprotein surface.** *FEBS Lett* 2003;**533**(1-3):21-4.
- <sup>30</sup> Shumaker VN, Puppione DL. **Sequential Floatation Ultracentrifugation.** *Methods in Enzymology* 1986;**125**:155-170.
- <sup>31</sup> Peterson, GL (1983) *Methods Enzymol.* 91, 95-119.
- <sup>32</sup> McNamara JR, Small DM, Li Z, Schaefer EJ. **Differences in LDL subspecies involve alterations in lipid composition and conformational changes in apolipoprotein B.** *J Lipid Res* 1996;**37**(9):1924-35.
- <sup>33</sup> Laemmli, UK. (1970) *Nature* 680, 227.
- <sup>34</sup> Esterbauer H, Striegl G, Puhl H, Rotheneder M: **Continuous monitoring of in vitro oxidation of human low density lipoprotein.** *Free Radic Res Commun* 1989, **6**(1):67-75.
- <sup>35</sup> Hurt E, Bondjers G, Camejo G: **Interaction of LDL with human arterial proteoglycans stimulates its uptake by human monocyte-derived macrophages.** *J Lipid Res* 1990, **31**(3):443-454.

- 
- <sup>36</sup> Mourao PA, Pillai S, Di Ferrante N: **The binding of chondroitin 6-sulphate to plasma low density lipoprotein.** *Biochim Biophys Acta* 1981, **674**(2):178-187.
- <sup>37</sup> Rifai, Nader, G. Russell Warnick, and Marek H. Dominiczak. Handbook of Lipoprotein Testing. 2<sup>nd</sup> ed. Amer. Assoc. for Clinical Chemistry. 2000.
- <sup>38</sup> Otvos JD, Jeyarajah EJ, Bennett DW, Krauss RM. **Development of a proton nuclear magnetic resonance spectroscopic method for determining plasma lipoprotein concentrations and subspecies distributions from a single, rapid measurement.** *Clin Chem* 1992;**38**(9):1632-8.
- <sup>39</sup> Campos H, Roederer GO, Lussier-Cacan S, Davignon J, Krauss RM. **Predominance of large LDL and reduced HDL2 cholesterol in normolipidemic men with coronary artery disease.** *Arterioscler Thromb Vasc Biol* 1995;**15**(8):1043-8.
- <sup>40</sup> Campos H, Moye LA, Glasser SP, Stampfer MJ, Sacks FM. **Low-density lipoprotein size, pravastatin treatment, and coronary events.** *Jama* 2001;**286**(12):1468-74.
- <sup>41</sup> Anber V, Griffin BA, McConnell M, Packard CJ, Shepherd J. **Influence of plasma lipid and LDL-subfraction profile on the interaction between low density lipoprotein with human arterial wall proteoglycans.** *Atherosclerosis* 1996;**124**(2):261-71.
- <sup>42</sup> Lada AT, Rudel LL. **Associations of low density lipoprotein particle composition with atherogenicity.** *Curr Opin Lipidol* 2004;**15**(1):19-24.
- <sup>43</sup> Galeano NF, Milne R, Marcel YL, Walsh MT, Levy E, Ngu'yen TD, Gleeson A, Arad Y, Witte L, al-Haideri M and others. **Apoprotein B structure and receptor recognition of triglyceride-rich low density lipoprotein (LDL) is modified in small LDL but not in triglyceride-rich LDL of normal size.** *J Biol Chem* 1994;**269**(1):511-9.
- <sup>44</sup> Nigon F, Lesnik P, Rouis M, Chapman MJ. **Discrete subspecies of human low density lipoproteins are heterogeneous in their interaction with the cellular LDL receptor.** *J Lipid Res* 1991;**32**(11):1741-53.
- <sup>45</sup> Galeano NF, Al-Haideri M, Keyserman F, Rumsey SC, Deckelbaum RJ. **Small dense low density lipoprotein has increased affinity for LDL receptor-independent cell surface binding sites: a potential mechanism for increased atherogenicity.** *J Lipid Res* 1998;**39**(6):1263-73.
- <sup>46</sup> Bjornheden T, Babyi A, Bondjers G, Wiklund O. **Accumulation of lipoprotein fractions and subfractions in the arterial wall, determined in an in vitro perfusion system.** *Atherosclerosis* 1996;**123**(1-2):43-56.

- 
- <sup>47</sup> de Graaf J, Hak-Lemmers HL, Hectors MP, Demacker PN, Hendriks JC, Stalenhoef AF. **Enhanced susceptibility to in vitro oxidation of the dense low density lipoprotein subfraction in healthy subjects.** *Arterioscler Thromb* 1991;**11**(2):298-306.
- <sup>48</sup> Garner B, Harvey DJ, Royle L, Frischmann M, Nigon F, Chapman MJ, Rudd PM. **Characterization of human apolipoprotein B100 oligosaccharides in LDL subfractions derived from normal and hyperlipidemic plasma: deficiency of alpha-N-acetylneuraminyl-lactosyl-ceramide in light and small dense LDL particles.** *Glycobiology* 2001;**11**(10):791-802.
- <sup>49</sup> Tertov VV, Sobenin IA, Orekhov AN, Jaakkola O, Solakivi T, Nikkari T. **Characteristics of low density lipoprotein isolated from circulating immune complexes.** *Atherosclerosis* 1996;**122**(2):191-9.
- <sup>50</sup> Tertov VV, Orekhov AN, Sobenin IA, Morrisett JD, Gotto AM, Jr., Guevara JG, Jr. **Carbohydrate composition of protein and lipid components in sialic acid-rich and -poor low density lipoproteins from subjects with and without coronary artery disease.** *J Lipid Res* 1993;**34**(3):365-75.
- <sup>51</sup> Anber V, Millar JS, McConnell M, Shepherd J, Packard CJ. **Interaction of very-low-density, intermediate-density, and low-density lipoproteins with human arterial wall proteoglycans.** *Arterioscler Thromb Vasc Biol* 1997;**17**(11):2507-14.
- <sup>52</sup> National Cholesterol Education Program. Third report of the expert panel on detection, evaluation, and treatment of high blood cholesterol in adults. NIH Pub. No. 02-5215. Bethesda, MD: National Heart, Lung, and Blood Institute, 2002;284 pages.
- <sup>53</sup> Rudel LL, Bond MG, Bullock BC. **LDL heterogeneity and atherosclerosis in nonhuman primates.** *Ann N Y Acad Sci* 1985;**454**:248-53.
- <sup>54</sup> Rudel LL, Parks JS, Johnson FL, Babiak J. **Low density lipoproteins in atherosclerosis.** *J Lipid Res* 1986;**27**(5):465-74.
- <sup>55</sup> Steele RH, Wagner WD, Rowe HA, Edwards IJ. **Artery wall derived proteoglycan-plasma lipoprotein interaction: lipoprotein binding properties of extracted proteoglycans.** *Atherosclerosis* 1987;**65**(1-2):51-62.
- <sup>56</sup> Ballinger ML, Nigro J, Frontanilla KV, Dart AM, Little PJ. **Regulation of glycosaminoglycan structure and atherogenesis.** *Cell Mol Life Sci* 2004;**61**(11):1296-306.



---

<sup>57</sup> Vijayagopal P, Srinivasan SR, Radhakrishnamurthy B, Berenson GS. **Interaction of serum lipoproteins and a proteoglycan from bovine aorta.** J Biol Chem 1981;**256**(15):8234-41.

<sup>58</sup> Little PJ, Tannock L, Olin KL, Chait A, Wight TN. **Proteoglycans synthesized by arterial smooth muscle cells in the presence of transforming growth factor-beta1 exhibit increased binding to LDLs.** Arterioscler Thromb Vasc Biol 2002;**22**(1):55-60.

<sup>59</sup> Owens RT, Wagner WD. **Proteoglycans produced by cholesterol-enriched macrophages bind plasma low density lipoprotein.** Atherosclerosis 1991;**91**(3):229-40.

### VITA

Wilma Ortega Espiritu was born on May 4, 1978, in Fairfield, California, and is an American citizen. She graduated from Salem High School in Virginia Beach, Virginia in 1996. She received her Bachelor of Science in Psychology from Virginia Tech in 2000. She received a Master of Science in Biochemistry from the Medical College of Virginia in Virginia Commonwealth University in 2005.